

Reduction and Aggregation of Silver Ions at the Surface of Colloidal Silica

Darren Lawless,[†] Sudhir Kapoor,[†] Pierre Kennepohl,^{†,‡} Dan Meisel,^{*,†} and Nick Serpone^{*,‡}

Chemistry Division, Argonne National Laboratory, Argonne, Illinois, 60439, and Department of Chemistry, Concordia University, Montreal, Canada H3G 1M8

Received: April 22, 1994; In Final Form: June 22, 1994[®]

The reduction of silver ions at the surface of 40 Å colloidal silica particles at pH 9 has been studied using the pulse radiolysis technique. The rate of reaction of e_{aq}^- with Ag^+ increases linearly with an increase in the Ag^+/SiO_2 ratio until a ratio of 12:1 is reached. At this loading the reaction becomes independent of the silver concentration at the particle surface. Ag^0 and Ag_2^+ , the first products of silver ion reduction in aqueous solution, have been identified by their absorption spectra as the primary species formed by the reduction of silver ions at the surface of SiO_2 . Within the time window of the experiments ($\leq 200 \mu s$) there is no evidence of larger silver cluster formations (e.g., Ag_4^{2+}) that are formed under identical conditions in the absence of silica. Evidently, the silica surface stabilizes the Ag_2^+ cation. Irradiation of Ag^+/SiO_2 solutions with trains of electron pulses leads to the formation of two small silver clusters exhibiting spectral bands at 290 and 330 nm and the conventional colloidal particle with its band at ~ 400 nm. These clusters are stable in the presence of oxygen for at least several weeks. Addition of redox active and reducing agents confirmed that the three spectral bands originate from three different clusters.

Introduction

The size-dependent chemical properties of various semiconductor and metallic particulates have been the subject of numerous recent studies.¹ Because of the technological importance of silver in heterogeneous reduction, and in particular in photographic processes, a considerable amount of attention has focused on the formation and properties of small silver clusters of varying size. The dynamics and coalescence of silver atoms into larger aggregates have been examined in aqueous solution,^{2,3} in micelles,⁴ in the gas phase,⁵ in cryogenic matrices,⁶ and at the surface of silver halide materials.^{7,8}

Colloidal silver particles often show a strong absorption maximum in the 380–400 nm region. The intensity and shape of this absorption maximum, which may be explained in terms of surface collective oscillations of the electrons in the metal, are highly sensitive to the environment surrounding the particle.⁹ For example, adsorption of SH^- groups at the surface causes broadening of the absorption band.¹⁰ These changes are reversible upon desorption of the SH^- . On the other hand, adsorption of cadmium ions results in a hypsochromic shift of the absorption band.¹¹ Furthermore, the position of the surface plasmon absorption of the silver particles differs from the discrete electronic excitations attributable to smaller silver clusters. In this respect, silver differs from copper¹² and gold colloids¹³ whose discrete excitations are superimposed on the surface plasmon absorption.⁹

In order to gain insight into the properties and the mechanism of silver cluster formation on a chemically inert support, we have undertaken to investigate the reduction of silver ions at the surface of negatively charged colloidal silica particles using the pulse radiolysis technique. Of particular interest here is the comparison between these processes in aqueous solution and at the surface of an oxide particle. Metal–support interactions are a well-known phenomenon in catalysis, and they might affect the reduction and aggregation processes. Further, it was recently

shown¹⁴ that large metallic silver colloids grown on Ag_2O interact with the support and cause a red shift in the surface absorption band. This shift was reversible upon dissolution of the Ag_2O and was attributed to partial charge transfer to the support. In the case of silica support, charge transfer from the silver clusters to SiO_2 is unlikely because of the wide band gap of the insulating SiO_2 . Nevertheless, surface OH^- groups may stabilize newly forming clusters and thereby alter their electronic and optical properties. The possibility that distinct clusters of silver will be formed at the surface of the silica is not unlikely considering that reduction of silver ions in the presence of polyanions, such as polyacrylate, has been shown to yield distinct Ag_n clusters with $n \leq 3$, with $3 < n \leq 10$, and with $n \gg 10$.^{15,16} These clusters are stable for long periods of time (hours to months). In this report we first examine the early stages of the reduction of Ag^+ on SiO_2 in order to determine the detailed mechanism of reduction; the second part of the paper explores the possibility that SiO_2 can stabilize larger silver clusters.

Experimental Section

All chemicals were of the highest purity commercially available and were used as received. A description of the chemical properties of the colloidal silica stock solution, as furnished by the manufacturer (NALCOAG 1115, Nalco Chemical Co.), used in this study is given below.

colloidal silica as SiO_2	15% w/w
pH	10.5
average particle diameter ($2r$)	40 Å
average surface area	750 m ² /g
specific gravity (at 68 °F) of the suspension	1.104
viscosity	10 cP

The concentration of the particles was deduced from eq 1.

$$[SiO_2]_p = [SiO_2]_M/\eta \quad (1)$$

The aggregation number, η , was calculated from the radius, r , of the silica particles (eq 2)

[†] Argonne National Laboratory.

[‡] Concordia University.

[®] Abstract published in *Advance ACS Abstracts*, September 1, 1994.

$$\eta = \frac{4\pi r^3 \delta}{3} \frac{N_0}{M_w} \quad (2)$$

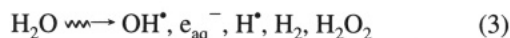
where N_0 is Avogadro's number and $\delta = 2.20 \text{ g/cm}^3$ is the density of silica. The particle concentration of the colloidal silica in the stock solution was calculated to be $3.4 \times 10^{-3} \text{ M}$. Silica concentrations in this report are given in terms of mole particles per liter.

Fresh stock solutions of $10^{-3} \text{ M AgClO}_4$, 10^{-2} M sodium borate, and 10^{-3} M silica particles were prepared prior to each pulse radiolysis experiment. The final borate concentration in all solutions was 10^{-3} M , resulting in solutions whose final pH was between 9 and 9.2. Solutions for pulse radiolysis study were prepared a day in advance and stirred in the dark overnight prior to deaerating by bubbling argon using the syringes technique. The amount of silver not adsorbed to the silica was determined by ultrafiltering the stirred solution through a Spectra/POR Type C filter (molecular weight cutoff of 5000; average pore size, $d_p = 15 \text{ \AA}$). The filtrate was then analyzed for silver by using atomic absorption.

Electron pulses, 2–40 ns in width, from the Argonne electron linear accelerator were used to produce between 2×10^{-6} and $2 \times 10^{-5} \text{ M}$ of e_{aq}^- per pulse. An aqueous, N_2O -saturated, solution of 10 mM KSCN was employed as the dosimeter [$G(OH^\bullet) = G(SCN)_2^{\bullet-} = 6.0 \text{ molecules/100 eV}$; $\epsilon_{480} = 7600 \text{ M}^{-1} \text{ cm}^{-1}$].

Results and Discussion

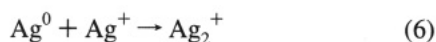
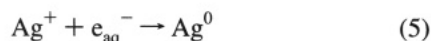
Irradiation of an argon-saturated aqueous solution with high-energy electrons generates principally $\bullet OH$, $H\bullet$, and solvated electrons (eq 3).



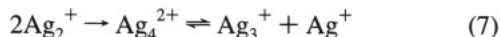
The *tert*-butyl alcohol contained in all solutions examined scavenged all the oxidizing hydroxyl radicals (reaction 4). The resulting *tert*-butyl alcohol radical is unreactive in this system and disappears via radical combination reactions.



The mechanism by which colloidal silver is formed in aqueous solution has been studied in some detail, the initial steps being (eq 5 and 6):



In solution, Ag_2^+ dimerizes to form Ag_4^{2+} or Ag_3^{2+} (reaction 7).^{17,18} The latter species was identified in zeolites as well.^{19–21}



Adsorption of Ag^+ at the Surface of SiO_2

Addition of silver ions to a colloidal solution of silica results in an equilibrium between the silver adsorbed at the SiO_2 surface (Ag_{ad}^+) and that free in solution (eq 8).



The equilibrium constant, $K = [Ag^+]_{ad}/[Ag^+][SiO_2]$, was determined from a plot of the amount of adsorbed Ag^+ versus the concentration of free silver in solution (determined following ultrafiltration). Several experiments were conducted in which

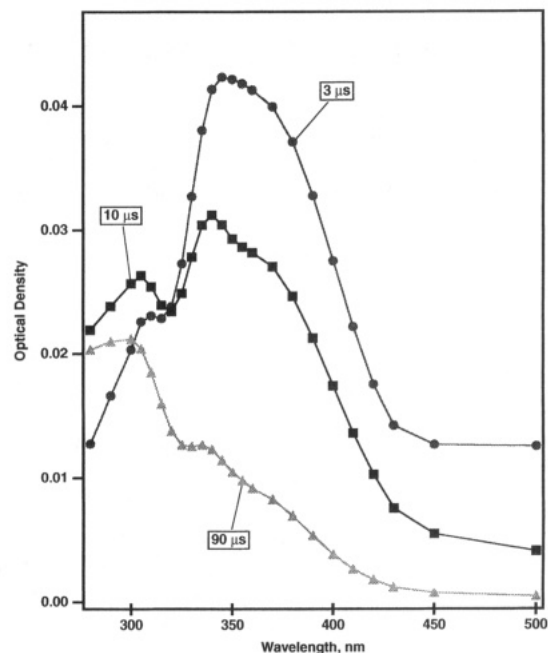


Figure 1. Absorption spectra of early transients formed after a 4 ns electron pulse in a solution containing $5 \times 10^{-5} \text{ M SiO}_2$, $2.5 \times 10^{-5} \text{ M Ag}^+$, 10^{-3} M sodium borate buffer (pH 9), and $0.1 \text{ M tert-butyl alcohol}$; $[e_{aq}^-]_0 = 6.0 \times 10^{-6} \text{ M}$.

the concentration of SiO_2 was held constant (1×10^{-5} or $1 \times 10^{-4} \text{ M}$) and the amount of silver added to the solution was varied (in the range 4×10^{-6} to $6 \times 10^{-5} \text{ M}$ or 4×10^{-5} to $6 \times 10^{-4} \text{ M Ag}^+$ for the two silica concentrations, respectively). In all cases, a good linearity between the amount of $[Ag^+]_{ad}$ and free Ag^+ in solution was observed; an average value of $K = (3.4 \pm 1.5) \times 10^5$ was obtained.

Reduction of Ag^+ at the Surface of SiO_2

The broad band gap ($\sim 10.5 \text{ eV}$) of the nonconducting SiO_2 precludes an electron transfer reaction from hydrated electrons to silica. Indeed, the decay rate of solvated electrons, followed by monitoring its absorption at 600 nm , was independent of SiO_2 concentration. Furthermore, in the absence of silver, no spectral features were observed, other than those attributable to e_{aq}^- .

Figure 1 shows the transient absorption spectrum of a solution containing $2.5 \times 10^{-5} \text{ M Ag}^+$, at an average of 1:2 Ag^+/SiO_2 ratio, following irradiation with a 4 ns electron pulse ($6.0 \times 10^{-6} \text{ M}$ of e_{aq}^- per pulse). An absorption band centered at approximately 360 nm forms following the pulse. This formation is complete within $3 \mu s$. Concomitant with the species growing in at 360 nm , a shoulder at approximately 315 nm also develops. The optical density of the species absorbing at 315 nm reaches its maximum approximately $10 \mu s$ after the pulse; at that time some of the initial absorption at 360 nm has already decayed. Clearly, the two absorption maxima arise from different species, and this fact is even clearer under the conditions of Figure 2. At longer times (Figure 1), both the 315 and 360 nm absorption maxima begin to decrease, although at different rates. As time progresses, there is an apparent blue shift of the absorption maxima originally centered at approximately 360 nm . This shift is due to the overlapping of the absorption spectra of the two absorbing transients, identified as Ag and Ag_2^+ , and is not related to any new absorbing species.

Increasing the average number of silver ions per silica particle to 4:1 leads to no new spectral features, indicating that within the time window of the experiment ($< 200 \mu s$) species such as

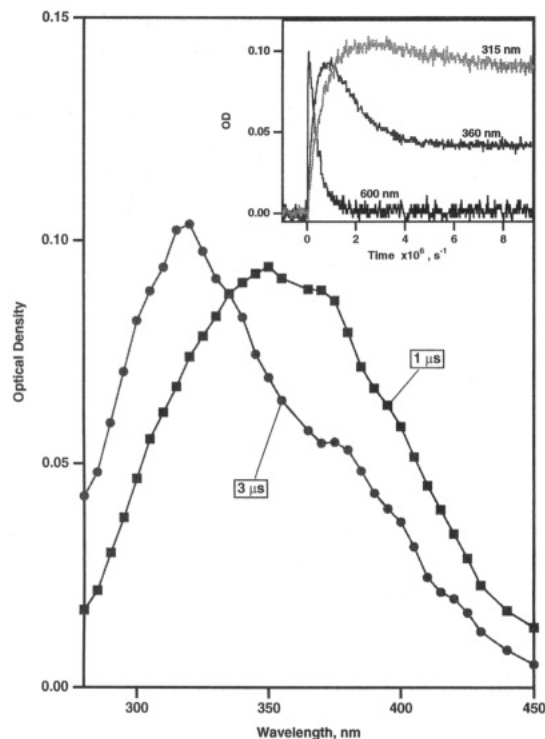


Figure 2. Absorption spectra of early transients formed after a 4 ns electron pulse in a solution containing 5×10^{-5} M SiO_2 and 2×10^{-4} M Ag^+ . All other concentrations are as in Figure 1. Inset: changes in optical density at 315, 360, and 600 nm with time.

Ag_4^{2+} ($\lambda_{\text{max}} = 275$ nm) are not formed. However, as the concentration of silver is increased, the absorbance maxima at 360 and 315 nm increase and their temporal resolution improves. At $[\text{Ag}^+]/[\text{SiO}_2]$ ratio of 4:1 (Figure 2) the absorbances at 360 and 315 nm is twice their values at a ratio of 1:2 (compare with Figure 1). The increased yield of reduction merely reflects the more efficient scavenging of e_{aq}^- at the higher Ag^+ concentration; at the lower $[\text{Ag}^+]$ a significant fraction of the ions are reduced. At the higher $[\text{Ag}^+]$ the absorbance at 360 nm reaches its maximum in less than 1 μs whereas the growth of the species that absorbs at 315 nm is complete within 3 μs (insert Figure 2). Formation of the species at 360 nm is concomitant with the electron decay (600 nm) in all cases. The decay of 315 nm transient, small as it is (20% of the total), is independent of the Ag^+/SiO_2 ratio, indicating that it is not an intraparticle reaction. The extinction coefficients at 360 and 315 nm are estimated to be 1.2×10^4 and 8.7×10^3 $\text{M}^{-1} \text{cm}^{-1}$, respectively, from Figure 2, assuming all e_{aq}^- are converted to Ag and then to Ag_2^+ . This is significantly lower than the values estimated for the same species in the bulk of the solution²² and may be a consequence of the presence of other pathways for disappearance of Ag than reaction 6 (e.g., formation of diatomic silver, but see below). However, we note that binding of Ag_2^+ to other species often leads to reduction in its extinction coefficient.⁴

No spectrum with $\lambda_{\text{max}} = 275$ nm, often attributed to Ag_4^{2+} , could be observed at times ≤ 200 μs . Therefore, one concludes that even at 200 μs after the pulse no dimerization of Ag_2^+ has occurred. When free in solution this reaction is complete on the same time scale. Thus, we further conclude that Ag_2^+ remains on the particle and does not desorb. Because the concentration of Ag_2^+ is much smaller than that of Ag^+ , its adsorption on the particles necessitates a larger adsorption equilibrium constant than for the parent ions. The reason for the stronger adsorption of Ag_2^+ than Ag^+ reflects the larger free

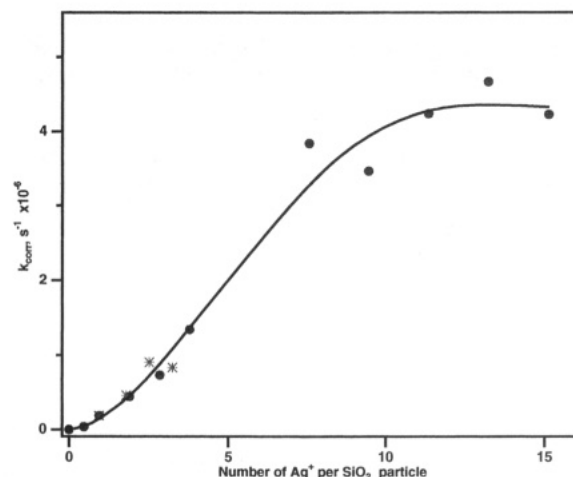


Figure 3. Rate constant for the reaction of e_{aq}^- with adsorbed Ag^+ measured at 600 nm as a function of $[\text{Ag}^+]/[\text{SiO}_2]$ ratio: (●) $[\text{SiO}_2] = 5 \times 10^{-5}$ M and $[\text{Ag}^+]$ varied; (*) $[\text{Ag}^+] = 5 \times 10^{-5}$ M and $[\text{SiO}_2]$ varied. All other concentrations are as in Figure 1.

energy for solvation of the latter; i.e., hydrophobic interaction between the former and the particle contributes to its adsorption.

Kinetics of Ag^+ Reduction and Early Cluster Formation

The reaction of the e_{aq}^- with Ag^+ may be conveniently followed at 600 nm. Using the equilibrium expression for reaction 8 and the average value of K , the concentration of free silver ions in solution was determined. From the known contribution of the free Ag^+ to the rate of the e_{aq}^- decay and from the knowledge of the natural lifetime of the electrons under the experimental conditions employed, the rate of the reaction of e_{aq}^- with adsorbed Ag^+ is then (eq 9)

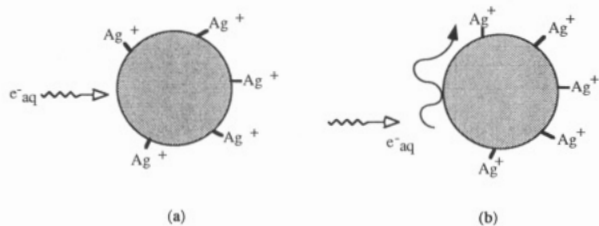
$$k_{\text{ad}} = k_{\text{obs}} - k_{\text{f}}[\text{Ag}^+]_{\text{f}} - 1/\tau_0 \quad (9)$$

where k_{obs} is the measured pseudo-first-order rate constant, k_{f} is the rate constant for free Ag^+ and was taken as 2.5×10^{10} $\text{M}^{-1} \text{s}^{-1}$, and τ_0 is the lifetime of e_{aq}^- ($=5.4 \times 10^5$ s^{-1}) in the absence of Ag^+ in these experiments.

Figure 3 shows the dependence of k_{ad} on the concentration of adsorbed Ag^+ . The latter was corrected for the amount of free ions using the adsorption constant as determined above. At $[\text{Ag}^+]/[\text{SiO}_2]$ ratios of approximately 12:1 the rate becomes independent of silver concentration at the silica surface. As can be seen in Figure 3, similar results were obtained when the $[\text{Ag}^+]/[\text{SiO}_2]$ ratio was varied holding either $[\text{SiO}_2]$ or $[\text{Ag}^+]$ constant. Varying the particle concentration over an order of magnitude (10^{-5} – 10^{-4} M) at a fixed $[\text{Ag}^+]/[\text{SiO}_2]$ ratio of 4:1 had no effect on the rate constant, k_{ad} .

The effect of the ratio $[\text{Ag}^+]/[\text{SiO}_2]$ on the observed first-order rate constant for the formation of the species absorbing at 315 nm (Ag_2^+) is similar to the one for Ag^+ reduction, and it parallels the dependence of the rate of the formation of Ag^0 at 360 nm. The first regime of Figure 3 was absent, but the rate increases on increasing $[\text{Ag}^+]$ at the SiO_2 surface and then levels off at approximately 12 Ag^+ ions per SiO_2 particle. The rate of formation of the species that absorb at 360 (Ag^0) and 315 nm (Ag_2^+) shows no significant dose dependence when the concentration of e_{aq}^- was varied by an order of magnitude. The observed decay at 360 nm was also dose independent and was identical, within experimental error, to the rate of formation of the absorption at 315 nm.

SCHEME 1: Two-Step Mechanism for the Reduction of Ag^+ at the Surface of SiO_2 . (a) Diffusion of Hydrated Electrons to the Particle; (b) Diffusion along the Surface to a Silver Ion



Mechanisms of Reduction and Cluster Formation

The first silver species that forms following the electron pulse has an absorption maximum at 360 nm. This species has been previously identified as Ag^0 . Three distinct regions can be observed in the S-shaped dependence of the rate of Ag^0 formation upon reduction of adsorbed Ag^+ by e_{aq}^- at the SiO_2 surface (Figure 3): (a) At low $[\text{Ag}^+]/[\text{SiO}_2]$ ratio the rate is low. In this region, however, the order of the reaction rate in $[\text{Ag}^+]$ is higher than one. (b) At intermediate ratios, k_{ad} is essentially linear with the concentration of Ag^+ at the surface. (c) The final region is where k_{ad} is independent of the amount of silver ions on the particle. These observations may be rationalized by considering the mechanism illustrated in Scheme 1. The reduction reaction is viewed as a two-step process: diffusion of e_{aq}^- to the particle (step a in Scheme 1) and diffusion of e_{aq}^- along the particle surface to encounter an adsorbed silver ion (step b). At low silver loading ($\text{Ag}^+/\text{SiO}_2 \leq 2$; first region in Figure 3), the rate-determining step is the diffusion of e_{aq}^- to the particle. In this process the electron needs to penetrate the negative potential field surrounding the silica particle (pH ca. 9), thus the slow rate of reaction in this regime. Increasing the concentration of adsorbed Ag^+ ions causes two effects. First, the probability of encountering a silica particle that carries an Ag^+ ion increases. Second, the negative surface potential at the plane of the reaction changes; it becomes more positive upon loading of additional silver ions. The combined effects are the reason for the strong dependence on $[\text{Ag}^+]$ at low loading. Above approximately two ions per particle, the electrostatic interaction between the surface and e_{aq}^- has been significantly diminished, and the diffusion to the particle is no longer the rate-determining step. It is the migration of e_{aq}^- along the particle surface to an adsorbed Ag^+ , step b in Scheme 1, that now determines the rate. This step is linearly proportional to the concentration of Ag^+ at the surface because the probability of encounter of e_{aq}^- with Ag_{ads}^+ increases with $[\text{Ag}^+]$. At yet higher Ag^+/SiO_2 ratio, the migration of e_{aq}^- along the surface to a silver ion is essentially instantaneous upon the arrival of e_{aq}^- at the particle. The diffusion of e_{aq}^- to the particle again becomes the rate-determining step, and thus the rate is independent of the loading at high ratios. For the 40 Å SiO_2 particle this plateau is reached at a Ag^+/SiO_2 ratio of approximately 12:1, and the bimolecular rate constant then is $8 \times 10^{10} \text{ M}^{-1} \text{ s}^{-1}$. This is essentially the rate constant for diffusion to the particles.

As Ag^0 decays, a new absorption feature with an absorption maximum at approximately 315 nm is formed. The absorption maximum of Ag_2^+ has been identified at 310 nm.²² The species at 315 nm cannot be the reaction product of two Ag^0 atoms because its formation shows no dose dependence. The dependence of its formation rate on $[\text{Ag}^+]$ suggests that the Ag^0 atoms react with Ag^+ ions. We, therefore, conclude that the second

step in the formation of silver clusters at the silica surface is the formation of Ag_2^+ (reaction 6) just as it is in aqueous solutions.

The fact that Ag_2^+ is formed even in systems where there is, on average, one or fewer silver ions per SiO_2 particle implies a desorption/adsorption mechanism for its formation. There are at least three mechanisms by which an exchange of Ag^+ or Ag^0 between two particles can occur.

1. A silica particle, containing an Ag^0 atom, encounters another particle that contains Ag^+ , subsequently leading to exchange of a silver species. Such an interparticle encounter and exchange is unlikely because the rate of formation of Ag_2^+ is faster than the diffusion-controlled rate for the encounter between two particles.

2. Desorption of Ag^0 occurs away from the silica particle on which it was formed followed by a reaction with a free Ag^+ ion in solution. This mechanism is precluded because the observed half-life for formation at 315 nm is more than 2 orders of magnitude shorter than the one predicted for reaction 6, considering the small amount of free Ag^+ in solution. For example, from $k_6 = 8 \times 10^9 \text{ M}^{-1} \text{ s}^{-1}$ ²² and the adsorption constant determined above, one calculates that the rate of such a reaction will be on the millisecond time scale at $[\text{SiO}_2] = 1 \times 10^{-4} \text{ M}$ and $\text{Ag}^+/\text{SiO}_2 = 0.5$. For the same reason, any mechanism that involves free Ag^+ could be precluded (e.g., desorption of Ag^+ followed by a reaction with adsorbed Ag^0).

3. Desorption of Ag^0 is followed by a reaction with an adsorbed Ag^+ ion on another SiO_2 particle. The latter is the most probable mechanism for the generation of Ag_2^+ at the SiO_2 surface. With this mechanism one expects, as observed, that the rate of Ag_2^+ formation becomes independent of Ag^+ loading at high Ag^+/SiO_2 ratio. At high loading the rate-determining step may then be either the desorption of Ag^0 or its encounter with another SiO_2 particle. However, in this regime the rate of Ag_2^+ generation becomes very similar to the rate of reduction of Ag^+ . Thus, the rate of the dimer formation is determined by the rate of its precursor formation. This means that the rate of desorption of Ag^0 is at least as fast as the rate of reduction at the plateau level of Figure 3. One, thus, concludes that Ag^0 desorbs very fast ($\tau_{1/2} \leq 100 \text{ ns}$; $k_{des}(\text{Ag}^0) \geq 7 \times 10^6 \text{ s}^{-1}$) from the surface of SiO_2 . Assuming that the adsorption of Ag^+ ions to the particles is a diffusion-controlled reaction ($k_{ads} \sim 5 \times 10^{10} \text{ M}^{-1} \text{ s}^{-1}$), one calculates $k_{des}(\text{Ag}^+) \sim 1.5 \times 10^5 \text{ s}^{-1}$ for the parent ions from the adsorption equilibrium constant. If one further assumes that the diffusion coefficients of Ag^+ and Ag_2^+ are similar, then $k_{des}(\text{Ag}_2^+) \ll 1.5 \times 10^5 \text{ s}^{-1}$, as we have already concluded that the latter is adsorbed more strongly. The order of stabilization of these three species on SiO_2 particles is $\text{Ag}^0 < \text{Ag}^+ < \text{Ag}_2^+$, and the rate of desorption is the one that determines their stability.

A striking difference between the growth of silver clusters in solution and at the surface of SiO_2 particles is that even at high silver ion loading there is no evidence for the formation of the characteristic absorption band of Ag_4^{2+} (or Ag_3^+ considering the ambiguity in its identification; $\lambda_{max} = 275 \text{ nm}$) at the surface of the silica particle. This is to be expected from the slow desorption and the high stability of Ag_2^+ at the surface as discussed above. However, at high silver loading at the silica surface, a new spectral feature at 360 nm grows during the first 20 μs after the pulse (Figure 4). As is clear from Figure 4, this species is neither Ag^0 nor Ag_2^+ . The observed growth followed pseudo-first-order kinetics and was independent of the Ag^+/SiO_2 ratio 6–20:1. Concomitant with this growth, the absorbance at 315 nm decays at the same rate. The new absorption can, therefore, be attributed to a silver cluster intermediate

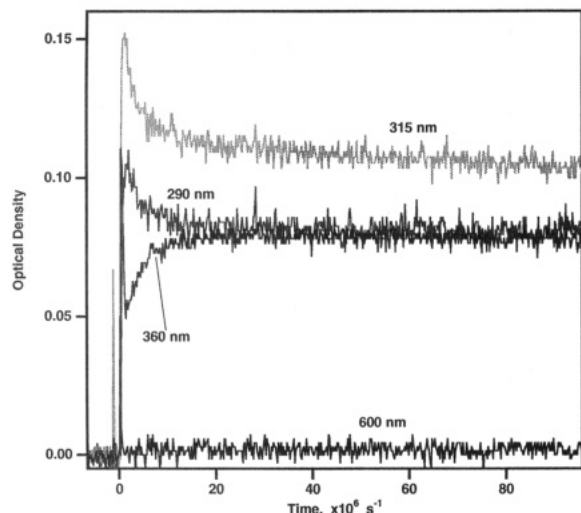


Figure 4. Changes in optical density as a function of time at various wavelengths following an electron pulse in a solution containing 5×10^{-5} M SiO_2 and 1.0×10^{-3} M Ag^+ , under conditions otherwise identical to Figure 1.

between Ag_2^+ and Ag_4^{2+} , possibly Ag_3^{2+} . A corollary of the kinetic analysis from above is that this species is formed by migration of Ag^+ ions and not the dimeric ion.

Long-Lived Silver Clusters at the Surface of SiO_2

During the past few years it has been shown that a variety of small silver clusters are stabilized by polyanions. The weak nucleophilic character of the anionic groups of the polyanion has been proposed as the binding force of these clusters to the polymer whereas the repulsive forces between polymer chains are thought to prevent intersegment agglomeration of the bound clusters.⁹ An analogous mechanism might also exist at the surface of colloidal silica; in such a case, the surface hydroxide groups of SiO_2 (and perhaps hydrophobic interactions as mentioned above) may bind the small silver clusters to the surface and the repulsive forces between particles may prevent agglomeration of the adsorbed clusters.

In order to determine whether silica is capable of stabilizing small silver clusters at the surface, samples were exposed to various radiation doses and the long-term stability of the generated clusters was studied. At relatively low doses, corresponding to $(0.2\text{--}2) \times 10^{-5}$ M e_{aq}^- , and at Ag^+/SiO_2 ratio of 1:1 ($\text{SiO}_2 = 5 \times 10^{-5}$ M), no silver clusters could be detected spectrophotometrically in the 250–700 nm region. However, when the dose was increased using trains of pulses (3×10^{-5} M e_{aq}^- per pulse) distinct long-lived clusters did develop. The inefficiency of agglomeration at low doses is attributed to the back-reaction of the initial clusters with the products of the oxidizing equivalents (e.g., *tert*-butyl alcohol radicals). At low doses, the highly reducing initial clusters are longer lived and the probability that they will react with the mildly oxidizing species is higher than at the high doses. For a similar reason, the efficiency of reduction was also dependent on the rate at which the dose was delivered to the parent solution. For example, when eight 40 ns pulses were applied over a 4 s time period, the absorbance of the bands attributed to silver clusters was triple their intensity following irradiation of an identical solution with an identical dose but delivered over 20 min.

Figure 5 illustrates the dependence of the absorbance of the clusters on dose. Three distinct absorption bands, at 290, 330, and 400 nm, can be seen in this figure, the higher wavelength band representing the stable, relatively large, well-established colloidal silver particles. As the number of electrons deposited

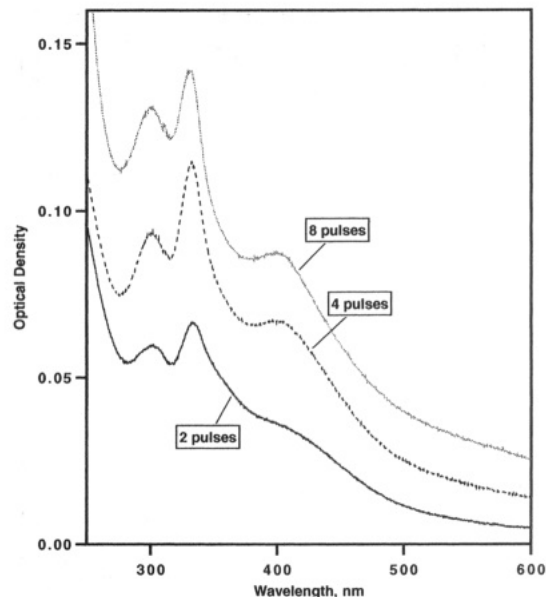


Figure 5. Absorption spectra of silver clusters formed 15 min after irradiating Ar-purged solutions containing 5×10^{-5} M SiO_2 and 5×10^{-5} M Ag^+ , under conditions otherwise identical to Figure 1, with varying number of pulses (40 ns pulse width, 3×10^{-5} M e_{aq}^- per pulse; 0.5 s between pulses).

into the system increases, the intensity of all three bands increases. In the absence of SiO_2 , the spectral bands at 290 and 330 nm were not observed; only the surface plasmon absorption band of colloidal silver was detected. Similar absorption bands have previously been observed upon reduction of silver ions in the presence of polyanions^{16,18} and were assigned to clusters of different sizes. Addition of 10^{-2} M NaClO_4 to the solution prior to irradiation did not affect the formation of all three spectral features. As noted above, Na^+ ions at that concentration displace Ag^+ ions from the surface of the silica particles. Thus, it may be concluded that the silver clusters whose spectra are given in Figure 5 originate from bulk species that adsorb onto the particles during the growth process. Once formed, the three spectral bands are not affected by addition of methyl viologen (except for slight coagulation), by admission of air, or by bubbling O_2 into the cell. On the other hand, addition of Cu^{+2} ions ($E^\circ = 0.15$ V NHE) or $\text{Ru}(\text{NH}_3)_6\text{Cl}_3$ ($E^\circ = 0.21$ V) to the solution also lead to the disappearance of the 290 nm band but have no effect on the other two absorption bands. These observations imply that the former clusters have their redox potential in the range of $0.15 > E_f > -0.33$ V. The latter clusters, however, are quite large, and their redox potentials approach that of the bulk material.²³

Despite the similarity in the redox potential of the species absorbing at 330 and 400 nm, they undoubtedly originate from two different species. This is evident from the changes that occur in the absorption spectra over a period of several weeks (Figure 6). The insert in Figure 6 shows the variation in the optical density as a function of time for the three spectral features. Initially (~ 10 min after the pulse), the 400 nm absorption is weak. After 4 days, the absorbance at this wavelength has nearly doubled while the absorbance at 290 and 330 nm has increased only slightly ($\approx 15\%$). Eventually, the band of the large colloidal particles increases and shifts to longer wavelength, at the expense of the smaller clusters that absorb light at the 290 and 330 nm bands. Clearly the three bands originate from different species.

The initial increase in absorbance during the first few days indicates that not all the silver ions have been reduced immediately after the pulse (despite the large excess of reduction

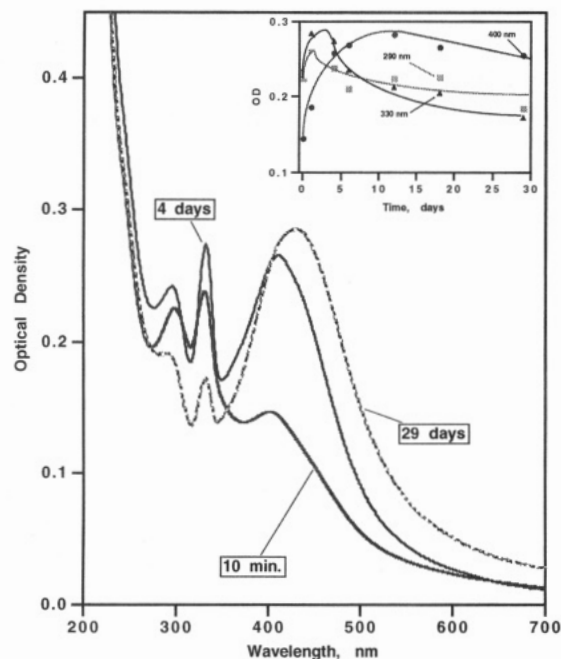


Figure 6. Changes in the absorption spectra of an irradiated solution, identical to the one shown in Figure 5, following eight electron pulses. Inset: changes in the absorbance with time at various wavelengths.

equivalents) and that a postirradiation reduction process occurs. The presence of unreduced Ag^+ ions in the irradiated solution was confirmed by the injection of H_2 -saturated solution to a cell containing the three silver cluster populations. Pronounced increase in the absorbance of the 290 and 330 nm bands was observed immediately thereafter. Generation of a reducing species under similar experimental conditions was confirmed upon irradiating to the same dose a solution containing an identical composition to that given in Figure 6 except for the Ag^+ ions. Addition of this irradiated solution to a solution containing 10^{-4} M silver ions led to the formation of relatively large colloidal silver particles within several days. Further, when a deaerated solution containing 10^{-4} M Ag^+ ions was added to the solution containing the silver clusters, all three spectral bands increased in intensity. The long-lived reducing species in these systems is most probably H_2 . Reduction of Ag^+ by H_2 is, thus, catalyzed by the presence of small silver particles but occurs slowly even in their absence.

Increasing the Ag^+/SiO_2 ratio from 1:1 to 4:1 resulted in several changes in the observed absorption spectra attributable to the presence of a larger concentration of Ag^+ ions and thus to acceleration of the growth process. With this higher concentration of Ag^+ , the efficiency of reduction is higher and the small clusters could be observed at lower doses. Similar absorption (in intensity and time evolution) to the one shown in Figure 6 was obtained with two 40 ns pulses delivered to this solution. On the other hand, when the dose exceeded the reduction equivalents required for complete reduction of the initial $[\text{Ag}^+]$, stabilization of the small clusters could not be achieved. This can be seen in Figure 7, where a solution containing 2×10^{-4} M Ag^+ , at a Ag^+/SiO_2 ratio of 4:1, was irradiated with five 3 μs pulses (1×10^{-4} M e_{aq}^- per pulse). Only residual absorption of small silver clusters can be observed in this figure, while the absorption of the colloidal particles continuously increases. The seemingly continuous blue shift reflects the addition of new, and smaller, particles rather than dissolution of large particles.

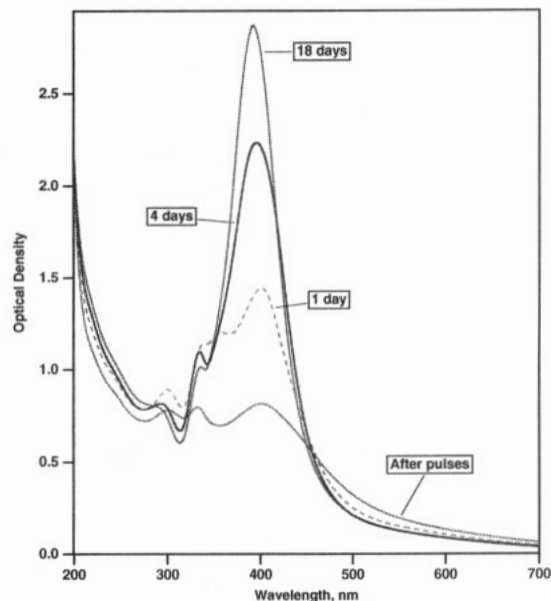


Figure 7. Changes in the absorption spectra with time of silver particles generated by irradiation of a solution containing 5×10^{-5} M SiO_2 and 2×10^{-4} M Ag^+ with five 3 μs pulses, under conditions otherwise identical to Figure 5.

Conclusions

A number of conclusions may be drawn from the present study. First, the dynamics of silver cluster formation at the surface of colloidal silica particles clearly differs from that in solution. The loading of the particles with silver ions has a pronounced effect on the agglomeration rates. Although Ag^0 and Ag_2^+ , the first products of silver ion reduction in aqueous solution, have been identified as the initial species formed upon reduction of silver ions at the surface of SiO_2 , larger silver clusters (e.g., Ag_4^{2+}) are much slower to form in the silica system than in the homogeneous solutions. Evidently the SiO_2 surface stabilizes the Ag_2^+ cation. The enhanced stability of these positive cationic clusters may divert the growth process to generate species that are usually not observed in aqueous solutions such as Ag_3^{2+} . The presence of the silica particles enhances the long-term stability of two oligomeric clusters of silver exhibiting spectral bands at 290 and 330 nm, in addition to the conventional colloidal particles that absorb at 400 nm.

Acknowledgment. Work at Argonne is performed under the auspices of the Office of Basic Energy Sciences, Division of Chemical Science, US-DOE, under Contract W-31-109-ENG-38. N.S. gratefully acknowledges support by the Natural Sciences and Engineering Research Council of Canada.

References and Notes

- (1) Henglein, A. *Top. Curr. Chem.* **1988**, *143*, 113.
- (2) Henglein, A. *J. Phys. Chem.* **1993**, *97*, 5457.
- (3) Henglein, A. *Chem. Rev.* **1989**, *89*, 1861.
- (4) Borgarello, E.; Pelizzetti, E.; Lawless, D.; Serpone, N.; Meisel, D. *J. Phys. Chem.* **1990**, *94*, 5048.
- (5) Hilpert, K.; Gingerich, K. A. *Ber. Bunsen-Ges. Phys. Chem.* **1980**, *84*, 739.
- (6) Stevens, A. D.; Symons, M. C. R. *J. Chem. Soc., Faraday Trans. 1* **1989**, *85*, 1439.
- (7) Mičič, O. I.; Meglic, M.; Lawless, D.; Sharma, D. K.; Serpone, N. *Langmuir* **1990**, *6*, 487.
- (8) Serpone, N.; Lawless, D.; Lenet, B.; Sahyun, M. R. V. *J. Imag. Sci. Technol.* **1993**, *37*, 517.
- (9) Henglein, A. *Isr. J. Chem.* **1993**, *33*, 77.

- (10) Mulvaney, P.; Linnert, T.; Henglein, A. *J. Phys. Chem.* **1991**, 95, 7843.
- (11) Henglein, A.; Mulvaney, P.; Linnert, T.; Holzwarth, A. *J. Phys. Chem.* **1992**, 96, 2411.
- (12) Ershov, B. G.; Janata, E.; Michaelis, M.; Henglein, A. *J. Phys. Chem.* **1991**, 95, 8996.
- (13) Mosseri, S.; Henglein, A.; Janata, E. *J. Phys. Chem.* **1989**, 93, 6791.
- (14) Huang, Z.-Y.; Mills, G.; Hajek, B. *J. Phys. Chem.* **1993**, 97, 11542.
- (15) Henglein, A.; Linnert, T.; Mulvaney, P. *Ber. Bunsen-Ges. Phys. Chem.* **1990**, 94, 1449.
- (16) Mostafavi, M.; Keghouche, N.; Delcourt, M.-O.; Belloni, J. *Chem. Phys. Lett.* **1990**, 167, 193.
- (17) Ershov, B. G.; Janata, E.; Henglein, A. *J. Phys. Chem.* **1993**, 97, 339.
- (18) Mulvaney, P.; Henglein, A. *Chem. Phys. Lett.* **1990**, 168, 391.
- (19) Gellens, L. R.; Mortier, W. J.; Schoonheydt, R. A.; Uytterhoven, J. B. *J. Phys. Chem.* **1981**, 85, 2783.
- (20) Michalik, J.; Zamadics, M.; Sadlo, J.; Kevan, L. *J. Phys. Chem.* **1993**, 97, 10440.
- (21) Ozin, G. A.; Hugues, F. *J. Phys. Chem.* **1983**, 87, 94.
- (22) Ershov, B. G.; Janata, E.; Henglein, A.; Fojtik, A. *J. Phys. Chem.* **1993**, 97, 4589.
- (23) Henglein, A. *Ber. Bunsen-Ges. Phys. Chem.* **1990**, 94, 600.